This article has been accepted for publication in a future issue of this journal, but has not been fully edited. Content may change prior to final publication. Citation information: DOI 10.1109/LAWP.2014.2388431, IEEE Antennas and Wireless Propagation Letters

Design and Full Characterization of Planar Active Magnetic RF Metamaterials

John P. Barrett, *Student Member, IEEE,* Steven A. Cummer, *Fellow, IEEE*

***Abstract*—Applications of metamaterials have been limited by parasitic resistive losses. We present the design and measurement of split ring resonators with embedded active field effect transistor circuits comprising a magnetic metamaterial. We show that the imaginary part of the effective permeability changes sign within the bandwidth of the negative differential resistance region, creating a stable gain medium. We present experimental reflection and transmission measurements showing a sign change in the permeability loss term and two applications of such a metamaterial: use as a mu-negative near field parasitic element for small magnetic antennas and as an amplifying material in free space. We show the active metamaterial can provide property enhancement compared with related passive structures in both applications, providing a path to overcoming parasitic loss in previously demonstrated metamaterial structures.**

I. Introduction

METAMATERIALS are structures that are composed of subwavelength unit cells that can form effective artificial materials with properties expressed in an unusual way compared with natural materials or not even readily found in nature. These unit cells can be formed by resonant structures such as split ring resonators (SRRs) and electric field coupling LC resonators (ELCs), which can express the unusual material properties of negative permeability [1], negative permittivity [2], and negative index of refraction [3]. Building on these properties and basic unit cells, other nonlinear behaviors have been demonstrated within metamaterials such as embedding diodes [4], power dependence [5], and phase conjugation [6].

These properties are also associated with high loss that are inherent to passive resonant structures. To overcome these limitations, active circuits and elements can be embedded in the unit cell. Previous attempts to try to mitigate the loss include embedding an amplifier [7]–[9] and using negative differential resistance (NDR) circuits [10]–[12] to cancel the parasitic resistances in the metamaterial unit cells. However, these approaches have only looked at unit cells that were transmission line based, had stability issues, or are volumetrically large (preventing dense packing of the unit cells). Another issue with passive resonant structures is the limited bandwidth. For completeness of reviewing active metamaterials, attempts to improve the functioning bandwidth for these metamaterial structures have been suggested and shown using embedded non-Foster circuits [13] [14].

SRRs can also act as near field resonant structures in antenna systems or as an antenna array in free space. Using an SRR as a near field resonant parasitic structure creates an external matching network between an electrically small antenna and free space [15], [16]. Within a finite bandwidth (specifically near the resonant frequency of the SRR), the electrically small antenna will operate more efficiently (Sec. III), resulting in an increase in radiated power.

The approach used here, which builds and extends upon [12], uses a single ended NDR circuit with a field effect transistor (FET). Bipolar transistors can also produce an NDR region within the context of the circuit used here, however, the biasing network for the FET is less complex. Our work moves beyond the previous work in several key ways. The unit cell in [12] was constructed using a 4 turn coil suspended out of the plane from where the circuitry is kept. Through this construction, the unit cell was characterized using circuit impedance, and its gain functionality was tested with reflection measurements alone.

In this work, we carry the concept towards metamaterial applications by increasing the frequency and reducing the unit cell to a planar structure for ease of material construction and incorporation of the active circuitry. More importantly, we performed a full effective material parameter characterization of the design with complete reflection and transmission measurements. These measurements show for the first time that the extracted material parameters show regions of $Re\{\mu_r\} < 0$ and we demonstrate the application of one of these SRRs as a near-field parasitic element.

With the active circuitry embedded within the SRRs, the individual elements essentially become active integrated antennas (AIAs). AIAs have been explored before using separate receiving and transmitting layers [17]. Using a metamaterial unit cell, the receiving and transmitting antennas become one and the same, allowing for an array of these antennas to be constructed without significant volumetric constraints, creating the medium. When functioning as an effective medium (or antenna array), the constituitive individual SRRs can receive and transmit signals as a single loop antenna [6].

II. Material Parameter Extraction

Building on the work in [12], a single FET is used to create an NDR circuit if the source is loaded with a resonating LC tank [12]. The real part of the effective gate impedance (resistance) will shift from positive to negative at the resonant frequency of the LC source tank. The lower frequency conductance zero denotes the lower edge of the NDR frequency band, demonstrating the operating frequency in which the circuit exhibits the potential to express gain or cancel loss.

J. P. Barrett and S. A. Cummer are with the Department of Electrical and Computer Engineering, Duke University, Durham, NC, 27708 USA e-mail: (johnbarrett@alumni.duke.edu).

Manuscript received June 06, 2014; revised November 07, 2014; accepted December 14, 2014.

This article has been accepted for publication in a future issue of this journal, but has not been fully edited. Content may change prior to final publication. Citation information: DOI 10.1109/LAWP.2014.2388431, IEEE Antennas and Wireless Propagation Letters

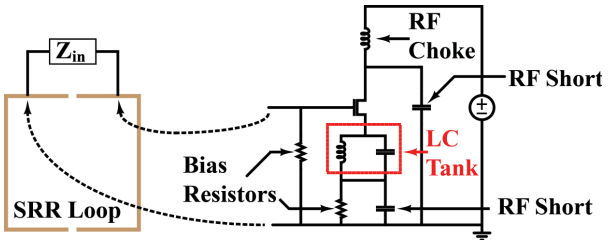

Fig. 1. Schematic of FET circuit [12] showing the embedded location in an SRR loop

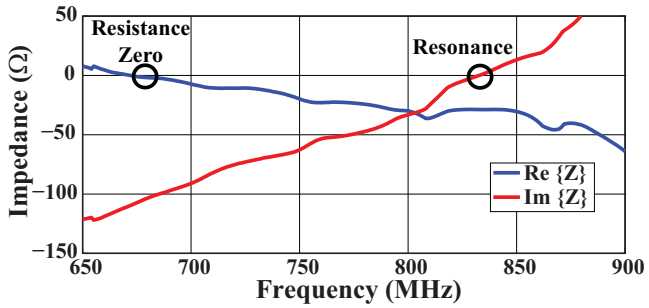

Fig. 2. Experimentally measured gate impedance (Z_{in} in Fig. 1). An additional 33nH inductor was placed in series between the gate and the measurement port.

To verify the NDR behavior (and to determine where the resistance zero is), the circuit was built using a NE3514S02 HJFET, an LC source tank resonance of 700MHz, and a 33nH inductor on the gate to stabilize the impedance measurement. The gate impedance was measured using a HP8720A vector network analyzer (VNA). Figure 2 shows an NDR region starting at 670 MHz. In order to stabilize the unit cell, the resonance and resistance zero must be properly tuned. These circuits also exhibit signficant variability between identical circuits due to manufacturing differences between fabricated transistors and other elements, but this is mitigated through the use of reactance and resistance tuning.

To show gain in a metamaterial medium, these circuits will need to be embedded in SRRs. Since that the SRR loop will add resistance and reactance, fabrication of the SRR requires careful selection of the SRR loop dimensions to provide the necessary loading impedance for stability while maintaining a strong magnetic response. The capacitive gap included in the loop ensures that the SRR will resonate as a magnetic unit cell and assists in shifting the resonance to a stable frequency.

Taking the relationship between circuit impedance and magnetic polarizability as seen in [12], the impedance term can be rewritten as $Z = R + jX$, where $R = R_{ring} + R_{circuit}$ and $X = \omega L_{ring} - \frac{1}{\omega C_{gap}} + X_{circuit}$. This relationship is rewritten as Eq. 1 to explicitly separate the real and imaginary terms.

$$\alpha = -\frac{\omega A^2 X}{R^2 + X^2} - j\frac{\omega A^2 R}{R^2 + X^2} \quad (1)$$

Looking at Eq. 1, the imaginary part of α changes sign and becomes positive when the operating frequency is within the NDR region. Converting the polarizability to the relative permeability preserves the positive sign from the polarizability loss term when the total resistance of the unit cell is negative, showing that the medium becomes a gain medium.

An SRR was fabricated with the proper loading reactance to have the resonance near the low frequency resistance zero. A potentiometer was placed at the transistor gate to provide tunability for the resistance zero, modulating the resistance curve and tuning the resonant frequency into a region of stability. This increase in resistance also decreases the bandwidth in which $\mathrm{Im}\{\mu_r\} > 0$.

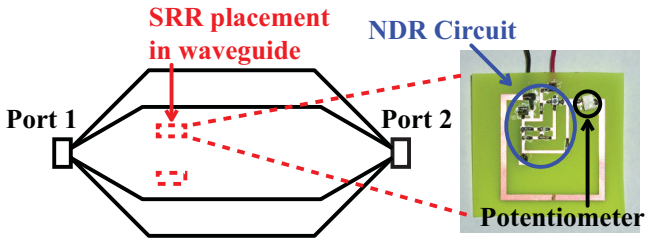

Fig. 3. Measurement setup for determining S-parameters and material response for medium of SRRs. The waveguide used was an open waveguide with 6 cm plate separation.

An SRR with the FET circuit as the loading element was fabricated to resonate near 700 MHz (Fig. 3) and tuned for stability. Looking at the SRR, the transistor circuit is placed in the inside of the loop, making the unit cell planar. This modification to an SRR can occur since none of the components are ferromagnetic, which means the presence of the circuit minimally affects the magnetic flux through the loop and the induced voltage. Stability of the SRR was checked up to 4 GHz by an external antenna connected to a spectrum analyzer, recording no signals above the noise floor.

The material response of the FET loaded SRR were measured using transmission and reflection S-parameter coefficients of a single active SRR unit cell and two active SRR unit cells in a waveguide (Figs. 3 and 4). The response of two passive SRR unit cells was also measured to provide comparison between the active and passive unit cells. It is important to note that at resonance, the active SRR resistance is positive to ensure stability.

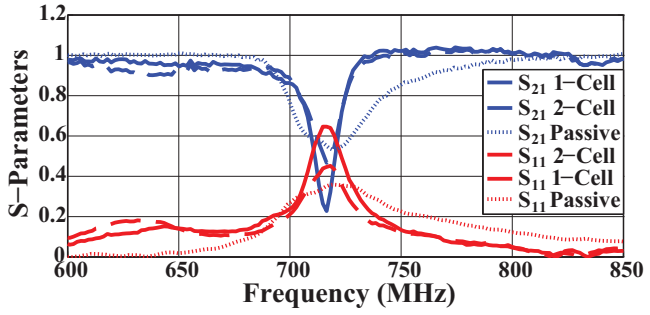

Fig. 4. Transmission and reflection S-parameters for a single unit cell, two active unit cells, and two passive unit cells.

.

.

There are significant differences in the S-parameters between the passive and active media. The responses for the

This article has been accepted for publication in a future issue of this journal, but has not been fully edited. Content may change prior to final publication. Citation information: DOI 10.1109/LAWP.2014.2388431, IEEE Antennas and Wireless Propagation Letters

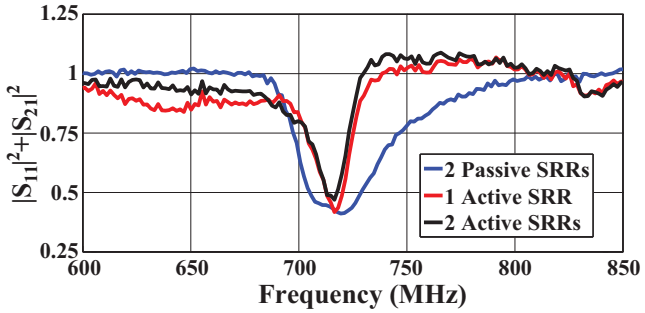

Fig. 5. Measured total system power (reflected power + transmitted power) for the metamaterial passive and active systems.

active unit cells demonstrate regions above the resonant frequency in which the transmission coefficient magnitude is greater than 1, while the passive unit cell response never has any parameters that exceed 1. The difference between the two transmission coefficient magnitudes demonstrates that only the active medium is providing gain. The active unit cells also have a deeper and narrower resonance than the passive unit cells, demonstrating loss cancellation. Another way to show the existence of gain within the system is through looking at the total power of the system (Fig. 5).

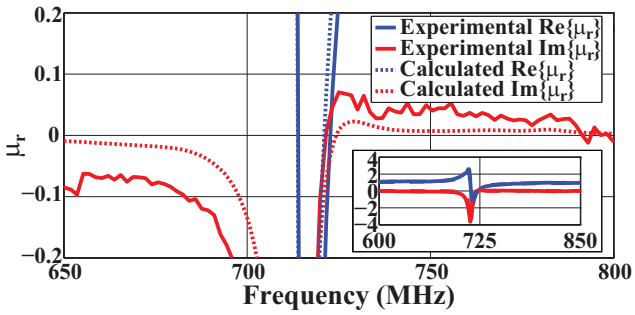

Fig. 6. Comparison of the experimentally extracted permeability with the calculated permeability based on measured impedance of the circuit with estimated inductance and capacitance values of the SRR loop.

To confirm the consistency between the measurements and the calculations based on the impedance curves of Fig. 2, the relative permeability of a fabricated active cell was extracted [7], [18], [19]. Looking at the comparison with the calculated permeability (Fig. 6), there is agreement between calculated and experimentally measured curves, confirming in both simulation and experiment that gain can be realized in the frequency regions where the resistance of the SRR unit cell is negative.

III. Free Space Measurements

The data shown in Fig. 6 reveals that these unit cells exhibiting MNG (μ-negative) and MNZ (μ-near-zero) behavior, we expect these unit cells to be able to provide some efficiency enhancement when used as a near-field parasitic (Fig. 7). For this experiment, an electrically small loop antenna was fabricated (diameter of 3.5 cm) and was connected to a port of the VNA used in Sec. II. The reflection coefficient measured by the VNA shows the efficiency of the antenna; if S_{11} is near 0 dB, then most (or all if S_{11}=0 dB) of the power supplied to the antenna is reflected back to the port and not transmitted into free space. From the measurements shown in Fig. 8, nearly 90% of the power is reflected back into the VNA port if the loop antenna is placed in free space without any impedance matching (the black curve).

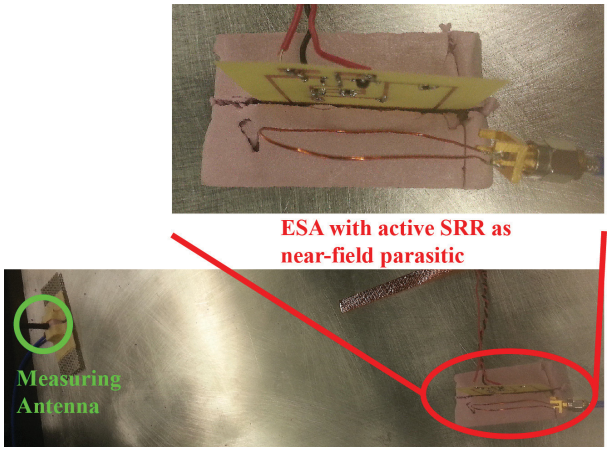

Fig. 7. Configuration and measurement setup for demonstrating the effectiveness of an SRR acting as a near-field parasitic. The spacing between the loop antenna and the SRR was 1 cm.

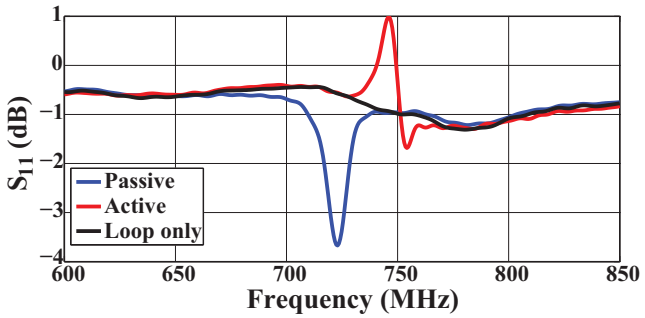

Fig. 8. Measurement of the reflection coefficient of the loop antenna using passive and active SRRs as near field parasitic elements as shown in Fig. 7.

TABLE I
MAXIMUM MEASURED FAR FIELD POWER ENHANCEMENT USING THE MEASUREMENT SETUP IN FIG. 7.

Maximum Power Enhancement	
Passive	Active
4 dB at 725 MHz	6 dB at 745 MHz

When a passive SRR is placed in the near field (the blue curve in Fig. 8), the reflection coefficient decreases over a finite bandwidth. This decrease in reflected power corresponds to more power is successfully radiating from the loop antenna, as measured by a separate antenna in the far field of the loop antenna/SRR system (Fig. 7 and Table I). When the active SRR replaces the passive SRR in the near field resonant parasitic system, the reflection coefficient curve changes from a region of decreased S_{11} to showing a region in which $S_{11} > 0$ dB,

This article has been accepted for publication in a future issue of this journal, but has not been fully edited. Content may change prior to final publication. Citation information: DOI 10.1109/LAWP.2014.2388431, IEEE Antennas and Wireless Propagation Letters

signifying the VNA is receiving more power than it originally transmitted. This is due to the active SRR producing gain in the coupled SRR/antenna. In conjunction with the results in Table 1, the active SRR also increases the radiative efficiency of the loop antenna as compared to the efficiency of the stand-alone electrically small antenna. The MNG/MNZ property of the SRR allows for more power to be transferred into free space, but some is absorbed by the SRR, amplified, and then re-emitted. The re-emitted energy is then sent back into the loop antenna or out into free space.

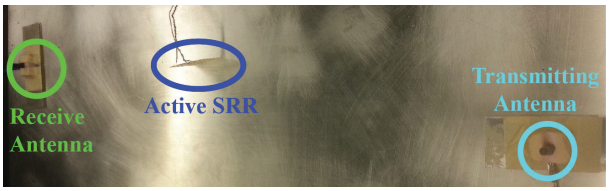

Fig. 9. Configuration and measurement setup for demonstrating the effectiveness of an SRR acting as a repeater. The SRR was 45 cm from both antennas.

To further demonstrate gain in free space using these SRRs as a metamaterial medium, the signal gain was measured looking at 3 signals with varying frequencies by placing the unit cell in between a transmitting and receiving antenna such that the SRR was in the far field of both antennas (Fig. 9). The active unit cell was tuned to have a resonant frequency of 693 MHz. The passive measurements were made with the medium in the off state (unpowered), as the unpowered unit cell does not affect signal transmission, and the active measurements were made with the cell in the on state (powered). The signal amplification (Table II) is consistent with previously measured shape of the imaginary part of the permeability curve. A maximum measured gain occurs close to the resonant frequency and falls off as the signal frequency moves away from the resonance. As expected given the material parameters, the gain will continue to fall off until the unit cell is transparent above the higher frequency resistance zero. As previously mentioned, there were no recorded oscillations below 4 GHz, confirming the stability of the circuit in this configuration.

TABLE II
MEASURED FAR FIELD GAIN FROM A SINGLE UNIT CELL USED AS A REPEATER.

Frequency	Gain
700 MHz	4.0 dB
720 MHz	3.2 dB
750 MHz	1.7 dB

IV. CONCLUSION

In conclusion, we have shown experimental data demonstrating the functionality of a transistor embedded active SRR. Experiments performed with single cell and two cell metamaterial media demonstrate MNG/MNZ behavior as well as free space signal amplification. The signal amplification and measured S-parameter coefficients are consistent with linear amplification below the transistor compression point. Future work includes providing additional tunability, increasing the bandwidth of the NDR region, and increasing the signal amplification through the metamaterial medium. The medium described has several potential applications in communication systems and other electromagnetic areas.

ACKNOWLEDGMENT

This work was supported by a Multidisciplinary University Research Initiative from the Army Research Office (contract no. W911NF-09-1-0539).

REFERENCES

[1] J. Pendry, A. Holden, D. Robbins, and W. Stewart, "Magnetism from conductors and enhanced nonlinear phenomena," *IEEE Transactions on Microwave Theory and Techniques*, vol. 47, no. 11, pp. 2075 –2084, nov 1999.

[2] D. Schurig, J. J. Mock, and D. R. Smith, "Electric-field-coupled resonators for negative permittivity metamaterials," *Applied Physics Letters*, vol. 88, no. 4, p. 041109, 2006.

[3] D. R. Smith, J. B. Pendry, and M. C. K. Wiltshire, "Metamaterials and negative refractive index," *Science*, vol. 305, no. 5685, pp. 788–792, 2004.

[4] C. Caloz, I.-H. Lin, and T. Itoh, "Characteristics and potential applications of nonlinear left-handed transmission lines," *Microwave and Optical Technology Letters*, vol. 40, no. 6, pp. 471–473, 2004.

[5] I. V. Shadrivov, A. B. Kozyrev, D. W. van der Weide, and Y. S. Kivshar, "Nonlinear magnetic metamaterials," *Opt. Express*, vol. 16, no. 25, pp. 20 266–20 271, Dec 2008.

[6] A. R. Katko, S. Gu, J. P. Barrett, B.-I. Popa, G. Shvets, and S. A. Cummer, "Phase conjugation and negative refraction using nonlinear active metamaterials," *Phys. Rev. Lett.*, vol. 105, p. 123905, Sep 2010.

[7] Y. Yuan, B.-I. Popa, and S. A. Cummer, "Zero loss magnetic metamaterials using powered active unit cells," *Opt. Express*, vol. 17, no. 18, pp. 16 135–16 143, Aug 2009.

[8] S. Gharavi and M. Mojahedi, "Theory and application of gain-assisted periodically loaded transmission lines with negative or superluminal group delays," in *Antennas and Propagation Society International Symposium, 2007 IEEE*, 2007, pp. 2373–2376.

[9] S. S. Oh and L. Shafai, "Compensated circuit with characteristics of lossless double negative materials and its application to array antennas," *Microwaves, Antennas Propagation, IET*, vol. 1, no. 1, pp. 29–38, 2007.

[10] A. D. Boardman, Y. G. Rapoport, N. King, and V. N. Malnev, "Creating stable gain in active metamaterials," *J. Opt. Soc. Am. B*, vol. 24, no. 10, pp. A53–A61, Oct 2007.

[11] W. Xu, W. J. Padilla, and S. Sonkusale, "Loss compensation in metamaterials through embedding of active transistor based negative differential resistance circuits," *Opt. Express*, vol. 20, no. 20, pp. 22 406–22 411, Sep 2012.

[12] L. Jelinek and J. Machac, "An fet-based unit cell for an active magnetic metamaterial," *Antennas and Wireless Propagation Letters, IEEE*, vol. 10, pp. 927 –930, 2011.

[13] S. Hrabar, I. Krois, and A. Kiricenko, "Towards active dispersionless enz metamaterial for cloaking applications," *Metamaterials*, vol. 4, no. 23, pp. 89 – 97, 2010.

[14] S. Hrabar, I. Krois, I. Bonic, and A. Kiricenko, "Negative capacitor paves the way to ultra-broadband metamaterials," *Applied Physics Letters*, vol. 99, no. 25, p. 254103, 2011.

[15] R. Ziolkowski, "Efficient electrically small antenna facilitated by a near-field resonant parasitic," *Antennas and Wireless Propagation Letters, IEEE*, vol. 7, pp. 581–584, 2008.

[16] R. Greegor, C. Parazzoli, J. A. Nielsen, M. H. Tanielian, D. C. Vier, S. Schultz, C. Holloway, and R. Ziolkowski, "Demonstration of impedance matching using a mu-negative (mng) metamaterial," *Antennas and Wireless Propagation Letters, IEEE*, vol. 8, pp. 92–95, 2009.

[17] J. Lin and T. Itoh, "Active integrated antennas," *Microwave Theory and Techniques, IEEE Transactions on*, vol. 42, no. 12, pp. 2186–2194, 1994.

[18] X. Chen, T. M. Grzegorczyk, B.-I. Wu, J. Pacheco, and J. A. Kong, "Robust method to retrieve the constitutive effective parameters of metamaterials," *Phys. Rev. E*, vol. 70, p. 016608, Jul 2004.

[19] B.-I. Popa and S. A. Cummer, "Compact dielectric particles as a building block for low-loss magnetic metamaterials," *Phys. Rev. Lett.*, vol. 100, p. 207401, May 2008.